



Prediction of proppant distribution as a function of perforation orientations

Shabeeb Alajmei^{1,2}

Received: 14 May 2023 / Accepted: 9 November 2023 / Published online: 12 December 2023
© The Author(s) 2023

Abstract

In treatments that involve multiple stages and clusters, one of the most important challenges is ensuring that the proppant is evenly distributed across all clusters. It is crucial to distribute the proppant equally to ensure that all perforation clusters are contributing to production. To forecast the proppant distribution between perforation clusters, an experimental correlation was established using data from the literature on horizontal wellbores. A dimensional analysis was performed using the Buckingham Pi-theorem to develop the correlation. Data from different independent variables, such as completion designs and orientations, were incorporated. In this study, an improved novel experimental correlation is proposed to accurately forecast the proppant distribution using various perforation configurations and orientations. The correlation can predict the proppant distribution with a low percentage difference of less than 20%. This correlation may be upscaled to predict the distribution of proppants across multiple clusters in a single-stage hydraulic fracturing stimulation. The developed correlation illustrates that injecting more proppant at a higher rate may help to allocate the proppant more evenly across perforation clusters. However, a nonuniform proppant distribution is obtained by increasing the proppant median diameter.

Keywords Proppant transport · Hydraulic fracturing · Unconventional reservoirs · Slickwater

Abbreviations

CFD Computational fluid dynamics
FR Friction reducer
GPM Gallon per minute
PPG Pound per gallon
SPF Shots per foot

μ Fluid viscosity, kg/m s
 ρ_p The solid particle density, g/cm³
 σ The standard deviation of proppant concentrations, kg/m³

List of symbols

C_p Proppant concentration, kg/m³
 D_p Average diameter of the particle, m
ID Inside diameter of the pipe, m
 n The number of the clusters, dimensionless
 N Number of perforations, dimensionless
PD Proppant distribution, %
 q Injection rate, m³/s
 s Arc length between the perforations, m
 \bar{X} The mean of the proppant concentrations, kg/m³

Introduction

The fracture conductivity associated with the placement of the proppant inside the induced fracture is one of the most influential factors affecting post-stimulation hydrocarbon production. The horizontal wellbore multistage hydraulic fracturing treatment can be optimized to boost production from unconventional sources. Distributing equal proppant concentrations across various perforation clusters completed within the same treatment stage of a horizontal well is crucial, yet it is considerably challenging. To assess the proppant distribution between different perforation clusters, a proppant distribution term (PD) is introduced. In this study, PD is technically defined as the percentage difference between the injected concentration of the proppant and the calculated standard deviation departed at different perforation clusters. As the standard deviation decreases, the proppant distribution (PD) increases and equals 100 for an ideal distribution between different perforation clusters (i.e., an

✉ Shabeeb Alajmei
alajmism@kfupm.edu.sa

¹ Department of Petroleum Engineering, King Fahd University of Petroleum & Minerals, 31261 Dhahran, Saudi Arabia

² Center for Integrative Petroleum Research, King Fahd University of Petroleum & Minerals, 31261 Dhahran, Saudi Arabia

even distribution). Several attributes affect the transport and distribution of proppants in a horizontal wellbore. These parameters include carrier fluid viscosity, injection rate of the slurry, horizontal wellbore internal diameter, completion design (i.e., number of shots per foot, SPF) and perforation orientation, and proppant characteristics such as density and size.

Numerous experimental and computational studies have been published recently to investigate the distribution and transport of proppants across different perforation clusters in a horizontal wellbore. Using a large-scale setup, Crespo et al. (2013) examined the behavior of proppant distribution in 2013. A 4-inch, 100-foot-long horizontal wellbore with three perforation clusters spaced 15 feet apart was used in their study. This investigation was numerically modeled by simulating many numerical scenarios using CFD (Bokane et al. 2013). These scenarios were generated by changing the carrier fluid viscosity, the slurry injection rate, and the proppant parameters. Smaller experimental horizontal wellbores have been used to continue the effort to comprehend the proppant distribution across different perforation clusters (Ahmad and Miskimins 2019; Alajmei 2022; Alajmei and Miskimins 2020, 2021, 2022; Ngameni et al. 2017). The industry is also striving to understand proppant transport beyond the horizontal wellbore into the induced hydraulic fractures experimentally and numerically (Alotaibi and Miskimins 2018; Bahri and Miskimins 2021; Brannon et al. 2006; Chang et al. 2017; Gadde et al. 2004; Sahai et al. 2014; Tatman et al. 2022; Wen et al. 2016; Woodworth and Miskimins 2007). The effect of varying the number of perforations and orientations on the proppant distribution was numerically investigated by Zhang and Dunn-Norman (2015). In their study, a constant injection rate of 2 bbl/min was used for each perforation, and the internal diameter of the perforation was 0.42 inch.

It has been reported that merely 30% of the completed perforations in tight formations do not account for hydrocarbon production (Miller et al. 2011). For optimal production, it is crucial to have thorough knowledge of the proppant distribution in the horizontal wellbore during hydraulic fracturing stimulation. Numerous studies have reported that proppant distribution behavior is highly influenced by the orientation of the perforation (Alajmei 2022; Alajmei and Miskimins 2020, 2022; Wu and Sharma 2016). Therefore, it is imperative to develop a more universal correlation that can predict proppant distribution when completing wells with different perforation designs and orientations. Sinkov et al. (2021) numerically simulated the proppant transport and settling in the horizontal wellbore. They found that the proppant distribution is more influenced by the number of perforations in the clusters than perforations' orientations. The proppant inertia associated with the injection rate is

another factor that significantly affects that proppant distribution (Wu and Sharma 2019).

This study provides an experimental correlation based on all available experimental tests on proppant transport using a horizontal wellbore, as previously reported in the literature (Ahmad 2020; Alajmei 2022; Alajmei and Miskimins 2020, 2021, 2022; Ngameni et al. 2017). The prediction of proppant behavior was modeled using a variety of hole configuration designs, expanding the scope of the previously available correlation (Alajmei 2023).

The experimental correlation presented in this study offers an optimization for proppant placement and distribution design in relation to variables such as the internal diameter of the horizontal wellbore, fluid viscosity, perforation orientation, number of perforations, injection rate and proppant concentration, and proppant size and density.

Experimental setups and data collection

The data used to develop and improve the experimental correlation in this study were obtained from the literature (Ahmad 2020; Alajmei 2022; Alajmei and Miskimins 2020, 2021; Ngameni et al. 2017). The primary component of the setup used to conduct all the experimental tests is a horizontal, translucent pipe that is approximately 30 feet in length and has three clusters of perforations, as shown in Fig. 1. The perforation design of these perforation clusters varies from 1 to 6 SPF, with multiple phasing designs from 0° to 180°. The design of the perforation diameter is 0.25 inches, and the length of each cluster is one foot. Two different internal diameters were used to examine the proppant distribution, including 1.5 inches and 2.5 inches. The primary purpose of these experimental tests is to assess the proppant movement and distribution using various pipe diameters and hole arrangements.

A three-bladed propeller is used to combine the proppant and water in the tank. After mixing for 10 min, the centrifugal pump is incorporated to inject a homogeneous slurry containing the proppant into the horizontal pipe. The pump is controlled using a variable frequency drive. The slurry injection rate is determined by placing a flow meter in the pipe after the pump. In addition, the pressure inside the pipe is constantly monitored by installing different pressure gauges before the perforation clusters. A brief description of the experimental process is shown in Fig. 2.

The correlation is derived by collecting all available published experimental data from the literature. Several parameters were employed as independent variables to establish this relationship, including type, size, and concentration of the proppant, fluid viscosity, injection rate, and number of perforations and their orientations. Data from various types of proppants were incorporated to develop the experimental

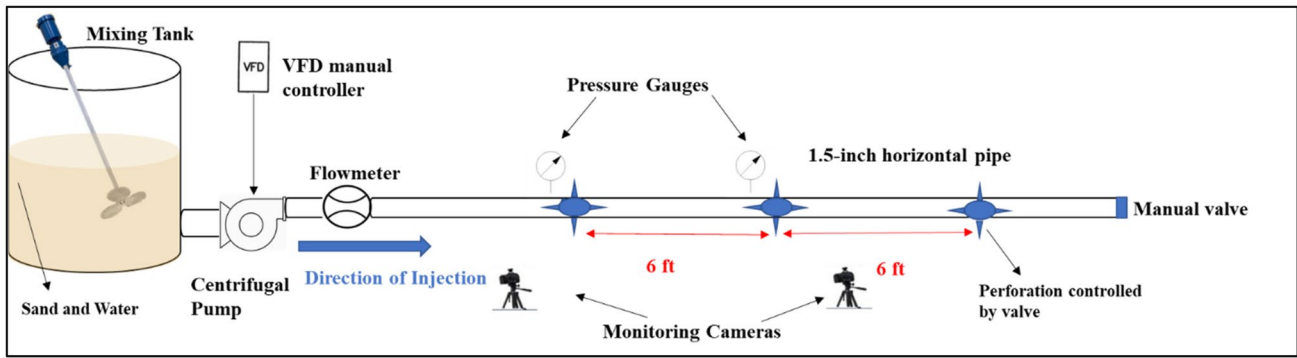


Fig. 1 Diagram of experimental setup (from Alajmei 2023)

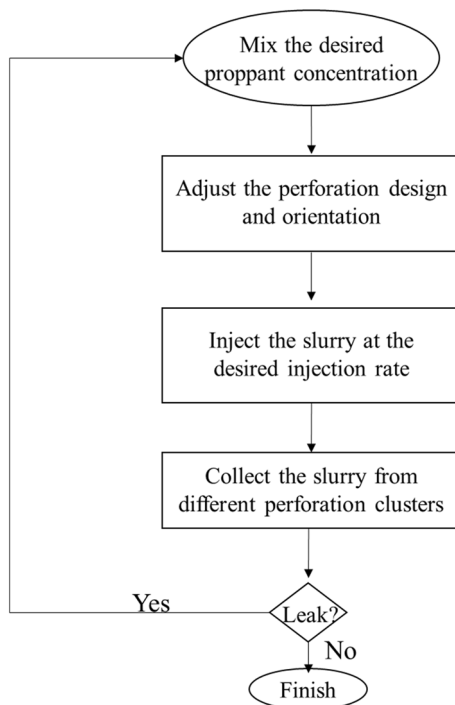


Fig. 2 Flowchart of experimental process

correlation, including sand with a specific gravity of 2.65 and ultra-light weight (ULW) ceramic with a specific gravity of 1.054 and 2.0. The size of the proppant used ranges from 100 mesh sand to 14/40 ULW, with proppant concentrations ranging from 0.07 ppg to 4.17 ppg. In this correlation, carrier fluid viscosities ranging from 1 to 17 cP and injection rates ranging from 0.001 m³/s to 0.005 m³/s were employed.

Correlation development methodology

The correlation is established by analyzing the effect of different parameters on the prediction of proppant distribution throughout multiple perforation clusters within a single hydraulic fracturing stage. Dimensional analysis was found to be an effective method for developing the correlation between various independent variables to forecast the dependent variable (i.e., proppant distribution) using the Buckingham (1914) Pi-theorem.

The diameter of the horizontal wellbore, the injection rate of the slurry, the concentration and density of the injected proppant, the average diameter of the proppant, the carrier fluid viscosity, the number of perforations, and the arc length between the perforations (i.e., orientation) were assigned as the independent variables used to establish the correlation.

To develop the correlation, three parameters, including fluid viscosity, pipe diameter, and proppant density, were selected as repeating variables. However, the remaining independent parameters, including the injection rate, the proppant size and concentration, the number of perforations open to flow, and the perforation orientation, were used as non-repeating variables. The Buckingham Pi-theorem constructs dimensionless correlations between the dependent and independent variables using Eq. (1).

The Buckingham Pi-theorem uses Eq. (1) to establish the correlation and forecast dependent variable (i.e., proppant distribution) using the input data of the independent variables.

$$\Pi_1 = \text{function}(\Pi_2, \Pi_3, \dots, \Pi_{n-k}) \tag{1}$$

where Π_1 is the dependent variable to be predicted (output); and $\Pi_2, \Pi_3, \dots, \Pi_{n-k}$ are the independent variables (input).

Proppant transport between perforation clusters (PD) is computed using real experimental data and then compared to the forecasted values. Equation (2) was used to calculate

the standard deviation of the measured (actual) proppant concentration drained from different perforation clusters.

$$\sigma = \sqrt{\frac{\sum(X - \bar{X})^2}{n}} \quad (2)$$

where σ is the standard deviation of all drained proppant concentrations, (kg/m³); \bar{X} is the mean of the proppant concentrations at different perforation clusters, (kg/m³); and n is the number of the clusters, dimensionless.

Then, the percentage difference between the actual injected proppant concentration and the standard deviation is calculated to determine the actual proppant distribution using the measured values in the laboratory. The standard deviation approaches zero, and the percentage difference approaches 100% when the proppant concentrations measured at the various perforation clusters are consistent (i.e., evenly distributed).

Buckingham's Pi-theorem requires all variables' SI units to be converted to fundamental dimensions (M, L, and T), as shown in Table 1.

For each Pi term, we randomly selected a set of repeating variables, whose number is equal to the number of previously determined dimensions. The following parameters are chosen as the repeating variables, which are the pipe internal diameter (ID), carrier fluid viscosity (μ), and proppant concentration (C_p).

To generate each Pi term's set of variables, first multiply each of the three repeating variables by one of the other non-repeating variables. Equation (3) displays a complete representation of the correlation generated by Pi-theorem.

$$\text{Proppant distribution, PD} = f\left(\frac{qC_p}{\text{ID}\mu}, \frac{D_p}{\text{ID}}, \frac{\rho_p}{C_p}, N, \frac{s}{\text{ID}}\right) \quad (3)$$

where PD is the forecasted proppant distribution, fraction, [M⁰ L⁰ T⁰]; q is the injection rate, m³/s, [M⁰ L³ T⁻¹]; C_p is the proppant concentration, kg/m³, [M¹ L⁻³ T⁰]; ID is the horizontal wellbore internal diameter, m, [M⁰ L¹ T⁰]; μ is

the viscosity of the carrier fluid, kg/m s, [M¹ L⁻¹ T⁻¹]; D_p is the median diameter of the proppant, m, [M⁰ L¹ T⁰]; ρ_p is the proppant density, kg/m³, [M¹ L⁻³ T⁰]; N is the number of perforations at each cluster, dimensionless; and S is the arc length between the open perforations, m, [M⁰ L¹ T⁰].

Using this dimensionless method, the original nine variables were successfully reduced to six. In order to evaluate the impact of the previously described Pi terms on the overall distribution of proppant, it was necessary to determine the Pi terms for each experimental test.

Tables 2, 3, 4, and 5 provide the tabulated findings of the calculated proppant distributions using actual laboratory experimental data and their associated injection rates and proppant concentrations.

The proppant distribution changes depending on a combination of independent factors. The size and density of the proppants, as well as the hole design, have a significant impact on proppant distribution because of the effects of gravity. The influence of gravity can be reduced by increasing the injection rate. Although it seems that increasing the viscosity of the fluid naturally leads to a more equal distribution of proppants, this is not necessarily the case; instead, an optimal combination of many independent variables must be achieved.

Equation 4 represents the experimental correlation derived from the findings of all the combined data in the literature by applying multilinear regression. The developed correlation combines all independent variables that influence the proppant distribution presented in Eq. 3, including proppant concentration (C_p), diameter (D_p) and density (ρ_p), injection rate (q), pipe diameter (ID), carrier fluid viscosity (μ), and perforation design (i.e., number of perforations (N) and arc length between the perforations (s)).

$$\text{PD} = 22.4 + 0.0015\left(\frac{qC_p}{\text{ID}\mu}\right) + 0.005\left(\frac{\rho_p}{C_p}\right) + 8.05N + 11.5\left(\frac{s}{\text{ID}}\right) - 876.7\left(\frac{D_p}{\text{ID}}\right) \quad (4)$$

Table 1 Converting the units of all variables from SI units to fundamental dimensions (Alajmei 2022)

Variable	SI unit	Dimension
Pipe diameter, ID	m	[M ⁰ L ¹ T ⁰]
Fluid viscosity, μ	kg/m.s	[M ¹ L ⁻¹ T ⁻¹]
Injection rate, q	m ³ /s	[M ⁰ L ³ T ⁻¹]
Proppant concentration, C_p	kg/m ³	[M ¹ L ⁻³ T ⁰]
Proppant median diameter, D_p	m	[M ⁰ L ¹ T ⁰]
Proppant density, ρ_p	kg/m ³	[M ¹ L ⁻³ T ⁰]
Number of perforation, N	–	[M ⁰ L ⁰ T ⁰]
Arc length, s	m	[M ⁰ L ¹ T ⁰]
Proppant distribution, PD	–	[M ⁰ L ⁰ T ⁰]

Data validations

The developed correlation was first validated using the data published by Ngameni et al. (2017). The model was tested against the most diverse possible experimental tests, utilizing a 6 SPF perforation design to guarantee its suitability over a wide range of independent variable combinations, as shown in Fig. 3. These experiments used various sizes and densities of proppant, using fresh water as the carrier fluid. The average proppant distribution of both the actual and

Table 2 Proppant distributions (PD) of various concentrations of 100-mesh sand at injection rates of 20, 30, and 40 gpm using fresh water (with a viscosity of $1 c_p$) as the carrier fluid (modified after Alajmei 2023)

Proppant type	Perforation design	Injection rate, gpm	Proppant concentration, ppg	Standard deviation, ppg	PD, %
100 mesh	1 SPF TOP	20	0.23	0.00	99.37
			0.61	0.00	99.71
			1.79	0.05	97.13
			2.82	0.09	96.69
		30	0.45	0.00	99.63
			1.59	0.03	98.23
			2.59	0.11	95.89
			0.81	0.01	99.12
		40	0.37	0.00	99.46
			0.82	0.01	98.35
			1.38	0.02	98.79
			2.00	0.03	98.72
	1 SPF bottom	20	0.30	0.25	16.88
			0.76	0.64	15.84
			1.48	0.93	37.03
			4.17	1.46	64.97
		30	0.44	0.20	54.24
			0.92	0.49	46.53
			2.91	1.24	57.52
			0.35	0.16	53.55
		40	0.65	0.48	26.14
			1.36	0.46	66.38
			0.13	0.06	52.23
			0.83	0.35	57.32
2 SPF top and bottom	20	1.92	0.61	68.32	
		3.28	0.70	78.58	
		0.48	0.07	85.63	
		0.96	0.15	84.40	
	30	2.03	0.48	76.14	
		0.33	0.03	90.76	
		0.67	0.03	94.94	
		1.35	0.04	97.40	
	40	1.84	0.05	97.17	

predicted values is approximately 79%, which represents a moderately even distribution between the different perforation clusters. Another validation method was performed by computing the residual of the proppant distribution, which is the difference between the actual proppant distribution derived from laboratory experiments and the predicted proppant distribution. The residual values range from -20% to 20% scattering at approximately 0%, with a mean of zero. In addition, the percentage difference between the actual and predicted proppant distributions was computed, resulting in a relatively low average percentage difference of 18%, as shown in Fig. 4.

In order to determine whether the generated correlation in Eq. 4 was valid for all experimental tests conducted on the proppant distribution in a horizontal wellbore, it

was compared with the observed proppant distribution, as shown in Fig. 5. With almost 200 data points, a significant correlation is found between the predicted and observed proppant distributions for all combinations of independent variables, with a multiple R value of 0.8. Consequently, the constructed model successfully predicts 80% of the proppant distribution in a horizontal wellbore for all published experimental data.

The proppant distribution may be reduced by increasing the average diameter of the proppant, leading to an unequal distribution of proppants. However, the proppant distribution across the perforation clusters becomes more uniform, as predicted by the established correlation, if the injection rate of the slurry and the concentration of proppants are both increased.

Table 3 Proppant distribution (PD) of various concentrations of 40/70 mesh sand at various injection rates and different fluid viscosities using different perforation designs

Fluid viscosity, c_p	Perforation design	Injection rate, gpm	Proppant concentration, ppg	Standard deviation, ppg	PD, %
1	1 SPF bottom	20	0.18	0.06	66.61
			0.29	0.17	40.72
			0.61	0.39	36.69
			1.70	0.66	61.06
		30	0.09	0.10	19.29
			0.48	0.27	43.70
			0.74	0.52	28.95
			1.08	0.70	35.02
	1 SPF top	40	0.24	0.17	28.24
			0.43	0.30	29.45
			0.55	0.45	19.27
			0.81	0.61	25.31
		30	0.22	0.09	57.73
			0.51	0.44	13.99
			0.67	0.49	26.27
			1.05	0.64	38.98
	2 SPF top and bottom	40	0.20	0.17	12.14
			0.41	0.34	18.54
			0.65	0.51	21.86
			1.17	0.76	35.31
		20	0.08	0.04	50.83
			0.23	0.13	42.57
			0.56	0.32	43.61
			1.33	0.34	74.47
3 SPF	30	0.24	0.09	60.49	
		0.49	0.23	52.19	
		0.68	0.27	61.16	
		1.23	0.43	64.57	
	40	0.15	0.07	52.82	
		0.38	0.19	48.98	
		0.50	0.24	51.69	
		0.71	0.29	58.79	
50	0.17	0.11	32.10		
	0.37	0.20	46.07		
	0.50	0.25	49.76		
	0.85	0.35	59.21		

Table 3 (continued)

Fluid viscosity, c_p	Perforation design	Injection rate, gpm	Proppant concentration, ppg	Standard deviation, ppg	PD, %	
	4 SPF	60	0.16	0.10	33.56	
			0.32	0.18	43.41	
			0.50	0.24	51.87	
			0.66	0.26	60.45	
		70	0.09	0.04	50.46	
			0.29	0.13	57.33	
			0.46	0.17	62.23	
			0.73	0.26	65.22	
		60	35	0.30	0.17	42.93
				0.37	0.23	36.59
				0.93	0.29	68.59
				1.10	0.36	67.32
	70		0.26	0.08	68.71	
			0.30	0.10	67.89	
			0.89	0.18	79.58	
			1.20	0.17	86.06	
	35	60	0.23	0.05	78.80	
			0.21	0.05	77.71	
			0.80	0.15	81.85	
			1.17	0.12	89.40	
		75	0.46	0.07	84.32	
			1.08	0.11	89.73	
			1.64	0.39	76.35	
			2.20	0.56	74.42	
60	60	0.39	0.07	82.71		
		0.94	0.04	95.41		
		1.25	0.11	91.12		
		2.10	0.13	93.93		
	75	0.45	0.07	83.77		
		1.02	0.12	88.22		
		1.20	0.13	89.32		
		1.80	0.15	91.44		
6 SPF	84	0.15	0.03	79.82		
		0.25	0.09	65.54		
		0.50	0.16	67.72		
		1.00	0.29	70.69		
		1.25	0.35	71.91		

Table 3 (continued)

Fluid viscosity, c_p	Perforation design	Injection rate, gpm	Proppant concentration, ppg	Standard deviation, ppg	PD, %
2.5	4 SPF	25	0.75	0.46	38.21
		45	1.00	0.43	57.43
		60	0.90	0.41	54.81
4.2	4 SPF	25	0.75	0.48	35.42
		45	1.00	0.47	52.95
		60	1.15	0.50	56.60
7.5	4 SPF	25	1.00	0.52	48.33
		45	1.25	0.54	57.02
		60	1.30	0.57	56.42
17	4 SPF	25	1.00	0.44	56.49
		45	1.00	0.50	49.51
		60	1.10	0.50	54.89

Discussion of the results

In this study, data from proppant transport experiments conducted between three clusters of perforations in a horizontal wellbore apparatus were used to establish a predictive correlation. The proppant distribution in horizontal wellbores during hydraulic fracturing operations may be affected by a number of factors, including perforation design, proppant size and density, and fluid viscosity. The correlation was developed through the use of dimensional analysis and Buckingham's Pi-theorem, considering all of the experimental data conducted on horizontal wellbores that are currently accessible in the published literature.

The newly developed correlation accurately predicted the proppant distribution behavior across different perforation clusters in most proppant distribution data. The correlation matched the data of the experiments conducted using a limited-entry perforation designs (i.e., 1 SPF, top perforation, 1 SPF, bottom perforation, and 2 SPF) testing two different sizes of sand with a specific gravity of 2.65. Furthermore, the correlation matched the proppant distribution conducted in the laboratory using a 3 SPF design and fresh water as the carrier fluid to transport two different sizes of sand. Another very reliable match was observed when using a perforation design of 4 SPF to investigate the distribution of three different sizes of sand (i.e., 100 mesh and 40/70 mesh). However, the model overestimated the data for the 20/40 mesh at low injection rates and underestimated the values at high injection rates. The developed model also underestimated

the proppant distribution values using the ultra-light weight ceramic proppants at different perforation designs of 4 SPF and 6 SPF. This could be attributed to the low specific gravity of these proppants. Finally, despite a very low proppant distribution value of approximately 2%, which could be attributed to an experimental error. The model matched the data of both tested sands using 4 SPF, friction reducers of different concentrations, and fresh water as the carrier fluids. The model has a high multiple R value of nearly 80%, indicating that it successfully fits the majority of proppant distributions found in the literature. If further experimental testing was conducted, particularly those using ultra-light weight ceramics on 4 SPF and 6 SPF perforation designs, the author feels that the model might be enhanced even further.

This correlation is developed based on experimental tests conducted primarily using slickwater fluids. Therefore, the prediction model was not tested using other carrier fluids such as guar. In addition, the correlation is derived from laboratory setups with smaller internal diameters than those used in the field. Furthermore, the pressure difference between the perforation clusters using the laboratory setups is negligible. Hence, the proppant distribution is not influenced by the pressure difference between the different clusters. Finally, the effect of gravity on the proppant distribution in the developed model is not incorporated. Consequently, the turbulence forces associated with the injection rates are assumed to be the main driving forces that enhance the capability of the carrier fluid to suspend the proppant.

Table 4 Proppant distribution (PD) of various concentrations of 20/40 mesh sand at various injection rates and different fluid viscosities using different perforation designs

Fluid viscosity, c_p	Perforation design	Injection rate, gpm	Proppant concentration, ppg	Standard deviation, ppg	PD, %
1	4 SPF	35	0.13	0.11	13.29
			0.12	0.11	11.65
			0.21	0.21	2.27
			0.31	0.25	17.92
			0.10	0.05	52.66
		60	0.12	0.07	41.97
			0.23	0.09	60.51
			0.36	0.10	73.12
			0.10	0.02	75.40
			0.07	0.03	63.26
		75	0.13	0.04	68.81
			0.31	0.10	67.75
			0.15	0.03	77.12
			0.25	0.09	63.36
			0.50	0.18	63.25
84	6 SPF	1.00	0.28	71.96	
		1.25	0.42	66.01	
		2.5	0.68	32.29	
		4.5	0.70	30.28	
		6.0	0.47	53.28	
4.2	4 SPF	25	0.50	0.51	2.24
		45	1.00	0.51	49.35
		60	1.25	0.57	54.77
7.5	4 SPF	25	0.75	0.45	39.94
		45	0.90	0.45	49.99
		60	1.00	0.47	53.43
17	4 SPF	25	1.00	0.68	31.63
		45	1.25	0.53	57.84
		60	1.50	0.66	56.15

Table 5 Proppant distribution (PD) of various concentrations of different ultra-light weight (ULW) proppants at various injection rates using fresh water (with a viscosity of 1 cp) as the carrier fluid at different perforation designs

Proppant size	Perforation design	Injection rate, gpm	Proppant concentration, ppg	Standard deviation, ppg	PD, %
20/40	4 SPF	35	0.30	0.17	43.62
			0.72	0.25	65.53
			1.14	0.34	70.60
			1.80	0.46	74.65
		60	0.21	0.08	60.99
			0.70	0.13	80.75
			0.94	0.26	72.58
			1.30	0.18	86.31
		75	0.21	0.04	80.88
			0.55	0.08	85.14
			0.85	0.11	87.31
			1.10	0.13	88.24
40/70	4 SPF	35	0.46	0.07	84.32
			1.08	0.11	89.73
			1.64	0.39	76.35
			2.20	0.56	74.42
		60	0.39	0.07	82.71
			0.94	0.04	95.41
			1.25	0.11	91.12
			2.10	0.13	93.93
		75	0.45	0.07	83.77
			1.02	0.12	88.22
			1.20	0.13	89.32
			1.80	0.15	91.44
14/40	6 SPF	23	0.30	0.57	90.76
		44	0.50	0.93	85.67
		57	1.00	1.54	54.50
		83	1.25	2.11	68.71
30/80		18	0.32	0.59	84.88
		44	0.50	0.93	85.47
		57	1.19	2.38	100.00
		83	1.60	3.03	89.65

Fig. 3 Data validation of the model using 6 SPF perforation design

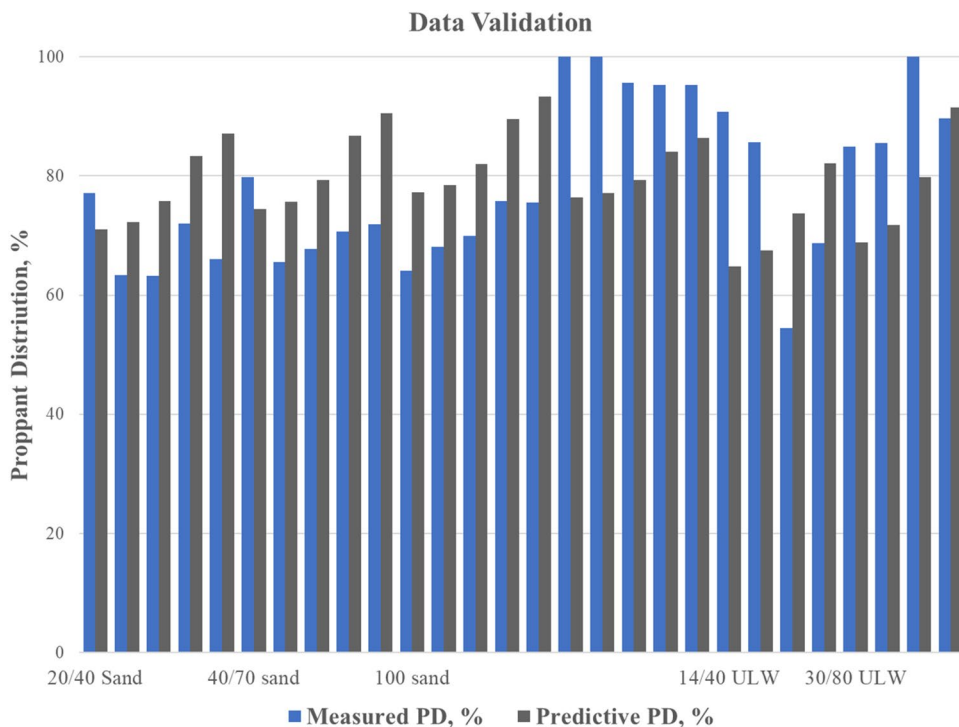


Fig. 4 Residual and percentage difference calculations between actual and predicted data

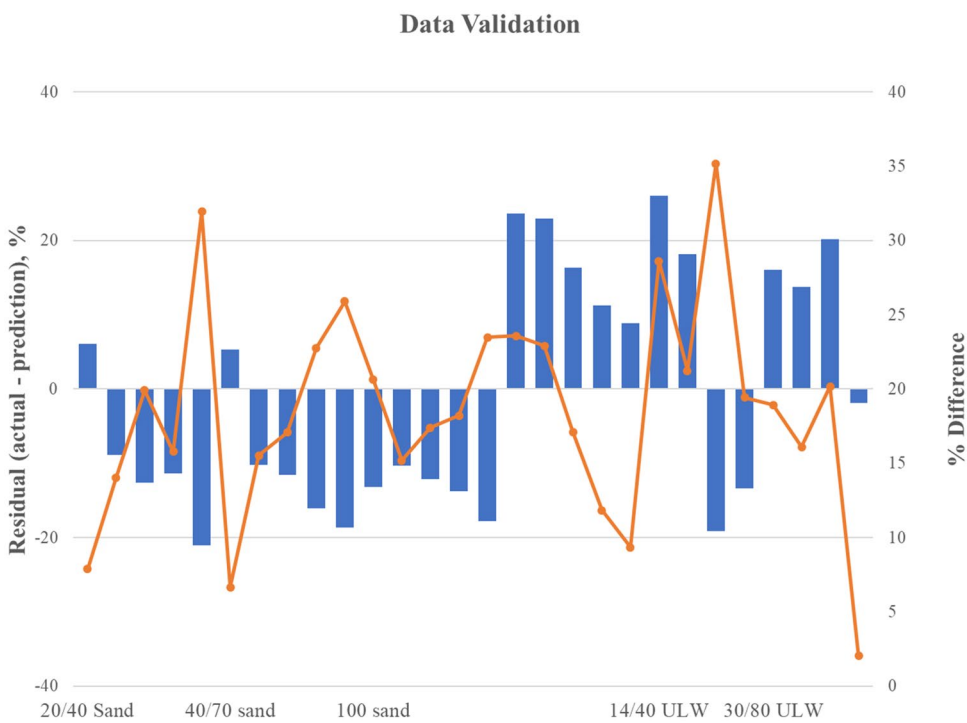
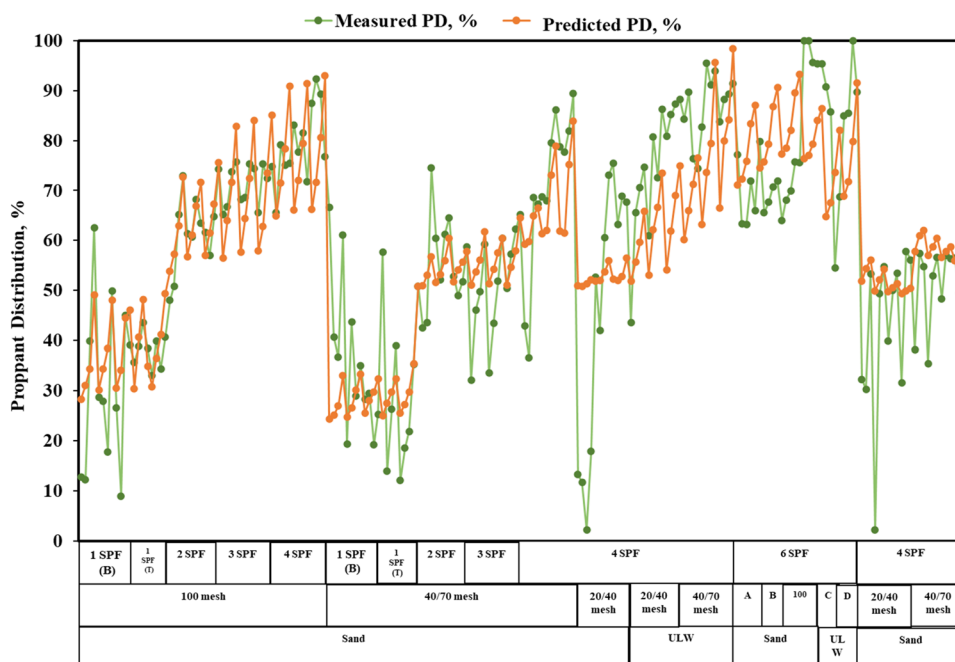


Fig. 5 Comparison of the predicted and the measured proppant distribution using different perforation designs and various proppant sizes and densities, **A** 20/49 sand, **B** 40/70 sand, **C** 14/40 ULW, and **D** 30/80 ULW



Conclusions

Conclusions that can be drawn from the established model for proppant distribution within a hydraulic fracturing stage include:

1. A correlation was created using all experimental data of proppant distribution tests on horizontal wellbores.
2. The proppant distribution is improved by increasing both the injection rate and proppant concentration. However, the proppant distribution is deteriorated with increasing particle diameter.
3. The established correlation offers a comprehensive correlation by incorporating a diverse set of experimental data and a broad variety of completions.
4. More experimental tests on ultra-light weight ceramics, particularly with 6 shot per foot and 4 shot per foot, can improve the correlation, significantly.

Acknowledgements The author acknowledges the support from the College of Petroleum Engineering and Geosciences (CPG) at King Fahd University of Petroleum and Minerals (KFUPM).

Funding No external funding was used.

Declarations

Conflict of interest The author declares no competing financial interest.

Open Access This article is licenced under a Creative Commons Attribution 4.0 International License, which permits use, sharing,

adaptation, distribution, and reproduction in any medium or format, as long as you give appropriate credit to the original author(s) and the source, provide a link to the Creative Commons licence, and indicate if changes were made. The images or other third-party material in this article are included in the article's Creative Commons licence, unless indicated otherwise in a credit line to the material. If material is not included in the article's Creative Commons licence and your intended use is not permitted by statutory regulation or exceeds the permitted use, you will need to obtain permission directly from the copyright holder. To view a copy of this licence, visit <http://creativecommons.org/licenses/by/4.0/>.

References

- Ahmad F (2020) Experimental investigation of proppant transport and behavior in horizontal wellbores using low viscosity fluids [Ph.D., Colorado School of Mines]. <https://search.proquest.com/docview/2413618582/abstract/5DE83D9A7C9D4720PQ/1>
- Ahmad FA, Miskimins JL (2019) Proppant transport and behavior in horizontal wellbores using low viscosity fluids. SPE Hydraul Fract Technol Conf Exhib. <https://doi.org/10.2118/194379-MS>
- Alajmei S (2022) Effect of variable perforation configuration on proppant transport and distribution using slickwater. <https://repository.mines.edu/handle/11124/15393>
- Alajmei S (2023) Proppant distribution prediction between perforation clusters using fresh water in a horizontal wellbore. ACS Omega. <https://doi.org/10.1021/acsomega.3c01696>
- Alajmei S, Miskimins J (2022) Effects of altering perforation configurations on proppant transport and distribution in freshwater fluid. SPE Prod Oper 37(04):681–697. <https://doi.org/10.2118/210573-PA>
- Alajmei S, Miskimins J (2020) Effects of variable perforation configurations on proppant transport and distribution in slickwater fluids. SPE Annu Technical Conf Exhib. <https://doi.org/10.2118/201605-MS>
- Alajmei S, Miskimins J (2021) Limited entry perforation configurations effect on proppant transport and distribution in fresh water. SPE Hydraul Fract Technol Conf Exhib. <https://doi.org/10.2118/204163-MS>

- Alotaibi MA, Miskimins JL (2018) Slickwater proppant transport in hydraulic fractures: new experimental findings and scalable correlation. *SPE Prod Oper* 33(02):164–178. <https://doi.org/10.2118/174828-PA>
- Bahri A, Miskimins J (2021) The effects of fluid viscosity and density on proppant transport in complex slot systems. *SPE Prod Oper* 36(04):894–911. <https://doi.org/10.2118/204175-PA>
- Bokane A, Jain S, Deshpande Y, Crespo F (2013) Computational fluid dynamics (CFD) study and investigation of proppant transport and distribution in multistage fractured horizontal wells. *SPE Reserv Charact Simul Conf Exhib*. <https://doi.org/10.2118/165952-MS>
- Brannon HD, Wood WD, Wheeler RS (2006) Large-scale laboratory investigation of the effects of proppant and fracturing-fluid properties on transport. *SPE Int Symp Exhib Form Damage Control*. <https://doi.org/10.2118/98005-MS>
- Buckingham E (1914) On physically similar systems; illustrations of the use of dimensional equations. *Phys Rev* 4(4):345–376. <https://doi.org/10.1103/PhysRev.4.345>
- Chang O, Dilmore R, Wang JY (2017) Model development of proppant transport through hydraulic fracture network and parametric study. *J Petrol Sci Eng* 150:224–237. <https://doi.org/10.1016/j.petrol.2016.12.003>
- Crespo F, Soliman M, Jain S, Bokane A, Deshpande Y, Kunnath Aven N, Cortez J (2013) Proppant distribution in multistage hydraulic fractured wells: a large-scale inside-casing investigation. *SPE Hydraul Fract Technol Conf*. <https://doi.org/10.2118/163856-MS>
- Gadde PB, Liu Y, Norman J, Bonnecaze R, Sharma MM (2004) Modeling proppant settling in water-fracs. *SPE Annu Tech Conf Exhib*. <https://doi.org/10.2118/89875-MS>
- Miller CK, Waters GA, Rylander EI (2011) Evaluation of production log data from horizontal wells drilled in organic shales. *North Am Unconv Gas Conf Exhib*. <https://doi.org/10.2118/144326-MS>
- Ngameni KL, Miskimins JL, Abass HH, Cherrian B (2017) Experimental study of proppant transport in horizontal wellbore using fresh water. *SPE Hydraul Fract Technol Conf Exhib*. <https://doi.org/10.2118/184841-MS>
- Sahai R, Miskimins JL, Olson KE (2014) Laboratory results of proppant transport in complex fracture systems. *SPE Hydraul Fract Technol Conf*. <https://doi.org/10.2118/168579-MS>
- Sinkov K, Weng X, Kresse O (2021) Modeling of proppant distribution during fracturing of multiple perforation clusters in horizontal wells. *SPE Hydraul Fract Technol Conf Exhib*. <https://doi.org/10.2118/204207-MS>
- Tatman G, Bahri A, Zhu D, Hill AD, Miskimins JL (2022) Experimental study of proppant transport using 3d-printed rough fracture surfaces. *SPE Annu Tech Conf Exhib*. <https://doi.org/10.2118/210196-MS>
- Wen Q, Wang S, Duan X, Li Y, Wang F, Jin X (2016) Experimental investigation of proppant settling in complex hydraulic-natural fracture system in shale reservoirs. *J Nat Gas Sci Eng* 33:70–80. <https://doi.org/10.1016/j.jngse.2016.05.010>
- Woodworth TR, Miskimins JL (2007) Extrapolation of laboratory proppant placement behavior to the field in slickwater fracturing applications. *SPE Hydraul Fract Technol Conf*. <https://doi.org/10.2118/106089-MS>
- Wu C-H, Sharma MM (2019) Modeling proppant transport through perforations in a horizontal wellbore. *SPE J* 24(04):1777–1789. <https://doi.org/10.2118/179117-PA>
- Wu C-H, Sharma MM (2016) Effect of perforation geometry and orientation on proppant placement in perforation clusters in a horizontal well. *SPE Hydraul Fract Technol Conf*. <https://doi.org/10.2118/179117-MS>
- Zhang J, & Dunn-Norman, S (2015) Computational fluid dynamics (CFD) modeling of proppant transport in a plug and perf completion with different perforation phasing. *SPE/AAPG/SEG unconventional resources technology conference*. <https://doi.org/10.15530/URTEC-2015-2169184>

Publisher's note Springer Nature remains neutral with regard to jurisdictional claims in published maps and institutional affiliations.